113 (20), 82 (86), 67 (100), 60 (12), 55 (14), 45 (50). The product was 94% ^{18}O by GC/SIM/MS analysis.

Synthesis of [8-^{18}O]-*exo*-Brevicomin. A. 2-[(*Z*)-4,5-Epoxyhept-1-yl]-2,5,5-trimethyl-1,3-dioxane (6). A solution of **5** (2.2 mmol) in CH_2Cl_2 (20 mL) was added to a vigorously stirred solution of $NaHCO_3$ (3.6 mmol) in water (7 mL). *m*-Chloroperbenzoic acid (MCPBA) (2.7 mmol) was added, and the biphasic system was stirred vigorously at room temperature overnight. Workup yielded a colorless oil (0.55 g, quantitative yield), 87% pure by GC analysis. ^1H NMR ($CDCl_3$): δ 0.88 (3 H, s, acetal methyl), 1.02 (3 H, s, acetal methyl), 1.04 (3 H, t, $J_{8,9}$ = 8 Hz, 9-H), 1.37 (3 H, s, 1-H), 1.47-1.78 (8 H, M, 3-H, 4-H, 5-H, 8-H), 2.84-2.90 (1 H, m, 7-H), 2.90-2.96 (1 H, m, 6-H), 3.42 (2 H, d, J_{gem} = 12 Hz, acetal methylenes), 3.56 (2 H, d, J_{gem} = 12 Hz, acetal methylenes). MS (EI) *m/z* (relative intensity): 227 (75), 129 (100), 69 (30).

B. [8-^{18}O]-*exo*-Brevicomin ([8-^{18}O]-1). Compound **6** prepared above (1.9 mmol), dissolved in anhydrous diethyl ether (~200 μL), was added to $^{18}OH_2$ (0.5 mL) through which gaseous HCl had been bubbled for ~10 s. The reaction mixture was stirred vigorously at room temperature, during which time aliquots were periodically removed and analyzed by GC. Gaseous HCl was periodically bubbled through the reaction mixture as needed to maintain a satisfactory reaction rate. After 12 h, the reaction was essentially complete. The two phases were separated, and the aqueous phase was extracted with 3 × 0.1 mL of anhydrous diethyl ether. The combined ether extracts were concentrated by blowing a gentle stream of argon over them. Bulb-to-bulb distillation under vacuum yielded crude ^{18}O-**1** (0.38 g) which was 70% pure by GC analysis. Purification by distillation under vacuum (69-72 °C, 20 mmHg) gave [^{18}O]-**1** as a colorless oil (0.25 g, 76% yield), which was 95% pure by GC analysis. ^1H NMR ($CDCl_3$): δ 0.91 (3 H, distorted t, $J_{10,11}$ = 7.5 Hz, 11-H), 1.41 (3 H, s, 9-H), 1.43-1.95 (8 H, m, 2-H, 3-H, 4-H, and 10-H), 3.93 (1 H, t, $J_{7,10}$ = 6.5 Hz, 7-H), 4.13 (1 H, br s, 1-H). ^{13}C NMR ($CDCl_3$): δ 9.61 (11-C), 17.15 (3-C), 25.00 (9-C), 28.00 and 28.58 (2-C and 10-C), 35.03 (4-C), 78.63 (1-C), 81.49 (7-C), 108.19 (5-C). MS (EI) *m/z* (relative intensity): 158 (M^+, 14), 129 (18), 116 (17), 114 (80), 101 (11), 100 (26), 88 (21), 87 (17), 85 (100), 81 (16), 72 (12), 68 (22), 67 (16), 45 (26), 43 (18).

The position of the ^{18}O label in the product was deduced from the ^{18}O-isotope-induced shifts of the ^{13}C NMR signals, after resolution enhancement of the ^{13}C NMR spectrum (line broadening, -0.5 Hz; Gaussian broadening, 0.3; 64K data set). The results are presented in Results and Discussion.

Registry No. (+)-**1**, 20290-99-7; [8-^{18}O]-**1**, 141171-85-9; (*Z*)-**2**, 34019-86-8; [^{18}O]-**2**, 141171-83-7; (6*S*,7*R*)-**3**, 141269-69-4; (6*R*,7*S*)-**3**, 141269-70-7; (*Z*)-**5**, 141171-84-8; (*S*,*R*)-**6**, 141269-71-8.

Cationic Metallovesicles: Catalysis of the Cleavage of *p*-Nitrophenyl Picolinate and Control of Copper(II) Permeation

Paolo Scrimin,* Paolo Tecilla, and Umberto Tonellato*

Contribution from the Department of Organic Chemistry and Centro CNR Meccanismi di Reazioni Organiche, University of Padova, Via Marzolo, 1, 35131 Padova, Italy.
Received September 3, 1991

Abstract: Ligand surfactants **1-3** have been synthesized. They feature a 2-(hydroxymethyl)pyridine as the ligand subunit and different lipophilic backbones which allow the formation, in aqueous solution, of different aggregates: vesicles in the case of **1** and **2**, micelles in the case of **3**. In the presence of Cu^{2+} ions, these aggregates are catalysts of the hydrolytic cleavage of activated esters of amino acids. Those made of surfactants **1** and **2** constitute one of the first examples of hydrolytic metallovesicles. The kinetic investigation was focused on the hydrolysis of the *p*-nitrophenyl ester of picolinic acid (PNPP): in line with previous results, the kinetic effects were attributed to the pseudo-intramolecular transacylation of a metal-ion-coordinated hydroxy group of the ligand subunit via the formation of a ternary complex comprising surfactant, Cu^{2+}, and PNPP. The observed accelerations were shown to be strongly dependent on the nature of the aggregate and, for vesicles, on the structure of the lipophilic backbone. This modulation of the reactivity has been attributed to (i) the different tendencies of the ligand amphiphiles in the aggregates to form nonproductive ternary complexes involving two ligand molecules and one Cu^{2+} ion and (ii) the rate of flip-flop of the surfactants which is suggested to be responsible for the transport of the Cu^{2+} ions across the vesicular membrane.

Synthetic liposomes[1] are the focus of the research interest of an increasing number of laboratories, as they may give information on critical phenomena pertaining to biological membranes.[2] The unique characteristics of a vesicular membrane, remarkably different from those of other assemblies, allow, for instance, the study of neutral and ionic molecular permeation,[3a] mobility of the surfactants in the bilayer,[3b] and catalytic efficiency[4] (in functional[5] aggregates). Furthermore, surface differentiation is possible, and indeed, several surface-differentiating reactions have been reported.[6] For instance, Moss and his associates have achieved chemical differentiation between the internal and external surfaces of a vesicle[7] through selective esterolysis. These authors have also shown how the intrabilayer movement (flip-flop) of the surfactant is dramatically dependent on the structure of the lipophilic backbone.[8]

The exciting outcome of new results in this area prompted us to broaden our interest on metalloaggregates[9] as mimics of hy-

(1) Fendler, J. H. *Membrane Mimetic Chemistry*; Wiley: New York, 1982; Chapter 6.
(2) Jain, M. *Introduction to Biological Membranes*, 2nd ed.; Wiley: New York, 1988.
(3) (a) Reference 2, Chapter 9. (b) Ibid., Chapter 4.
(4) Review of functional vesicles: Fuhrhop, J.-H.; Mathieu, J. *Angew. Chem., Int. Ed. Engl.* **1984**, *23*, 100.
(5) (a) Moss, R. A.; Scrimin, P.; Bhattacharya, S.; Swarup, S. *J. Am. Chem. Soc.* **1987**, *109*, 6209. (b) Moss, R. A.; Ganguli, S. *Tetrahedron Lett.* **1989**, *30*, 2071. (c) Kunitake, T.; Ihara, H.; Okahata, Y. *J. Am. Chem. Soc.* **1983**, *105*, 6070. (d) Murakami, Y.; Nakano, A.; Yoshimatsu, A.; Fukuya, K. *J. Am. Chem. Soc.* **1981**, *103*, 728.
(6) (a) Fuhrhop, J.-H.; Bartsch, H.; Fritsch, D. *Angew. Chem., Int. Ed. Engl.* **1981**, *20*, 804. (b) Tundo, P.; Kurihara, K.; Kippenberger, J.; Politi, M.; Fendler, J. H. *Angew. Chem., Int. Ed. Engl.* **1982**, *21*, 81. (c) Mizutani, T.; Whitten, D. G. *J. Am. Chem. Soc.* **1985**, *107*, 3621. (d) Kunitake, T.; Okahata, Y.; Yasunami, S. *J. Am. Chem. Soc.* **1982**, *104*, 5547.
(7) (a) Moss, R. A.; Bhattacharya, S.; Scrimin, P.; Swarup, S. *J. Am. Chem. Soc.* **1987**, *109*, 5740. (b) Moss, R. A.; Swarup, S. *J. Am. Chem. Soc.* **1986**, *108*, 5341.
(8) (a) Moss, R. A.; Bhattacharya, S.; Chatterjee, S. *J. Am. Chem. Soc.* **1989**, *111*, 3680. (b) Moss, R. A.; Ganguli, S.; Okumura, Y.; Fujita, T. *J. Am. Chem. Soc.* **1990**, *112*, 6391.

0002-7863/92/1514-5086$03.00/0

Scheme I[a]

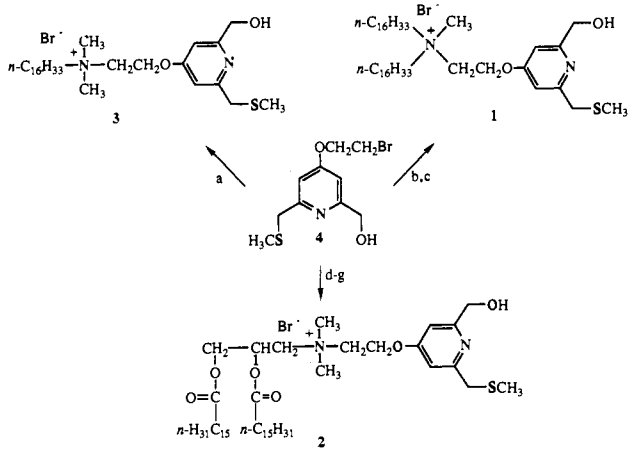

[a] (a) n-$C_{16}H_{33}N(CH_3)_2$, MeCN, 80 °C; (b) n-$C_{16}H_{33}N(CH_3)$, (i-Pr)$_2$EtN, MeCN, 80 °C; (c) n-$C_{16}H_{33}Br$, MeCN, and EtOH, 80 °C; (d) THP, PPTS, CH_2Cl_2, room temperature; (e) 3-(dimethylamino)-1,2-propanediol, MeCN, 80 °C; (f) n-$C_{15}H_{31}COOH$, DCC, DMAP, CH_2Cl_2, room temperature; (g) HCl, MeOH, room temperature.

drolytic metalloenzymes, on going from micelles to vesicles. We are pleased to report here our results with the ligand-functionalized cationic amphiphiles **1** and **2** which, in the presence of Cu^{2+} ions, constitute one of the first examples of hydrolytic metallovesicles.[10] The micelle-forming surfactant **3** was also studied for comparison. The *p*-nitrophenyl ester of picolinic acid (PNPP) was the substrate of choice. PNPP is a very sensitive probe of Cu^{2+} availability, as its rate of hydrolysis is strongly influenced by this metal cation.[11]

We will particularly address the question of the catalytic efficiency of metallovesicles as compared to that of metallomicelles and of the metal ion permeation across different vesicular membranes.

Results and Discussion

Synthesis and Properties of the Ligands. The key compound used for the synthesis of the ligand subunit of the three surfactants was the diethyl ester of chelidamic acid. This was elaborated (see Experimental Section) to obtain 4-[(2-bromoethyl)oxy]-2-(hydroxymethyl)-6-[(methylthio)methyl]pyridine (**4**), the intermediate used for the synthesis of all surfactants (see Scheme I).

Cationic amphiphiles **1–3** present common structural features: (i) the pyridine ring as the main ligand subunit of the system; (ii) the hydroxymethyl group which may be activated[9a] in the presence of Cu^{2+} (and Zn^{2+} as well[12]), to act as an effective nucleophile for the cleavage of PNPP; (iii) the thioether moiety suitable for monitoring Cu^{2+} complexation[13] (see below). They differ for the lipophilic portion: **3** has a single hydrocarbon tail, while **1** and **2** have two of them. Furthermore, in **1** the two chains are directly connected to the ammonium group, while in **2** they are connected via a glyceryl diester backbone resembling that of natural phospholipids.

Dispersion of surfactants **1** and **2** in water requires sonication which leads to the formation of aggregates, likely vesicles, detected by dynamic light scattering measurements. The size distribution of these aggregates as suggested by the Gaussian analysis of the light scattering data (see Table I) is rather broad and could indicate the coexistence of unilamellar[14] and bilamellar vesicular structures. However, several different preparations were quite reproducible in terms of size and kinetic behavior (see below). More definite evidence of the formation of closed vesicular aggregates in the case of **1** and **2** was obtained by trapping experiments using cationic ethidium bromide, EB, as a probe.[15] These experiments, as reported in detail in the Experimental Section and illustrated in Figures S1 and S2 of the supplementary material, show the fluorescence and scattered light intensity of EB loaded vesicles after gel permeation chromatography. Surfactant **3**, on the other hand, is reasonably soluble in water where it forms micellar aggregates.

The physical properties of the aggregates made of the above amphiphiles are reported in Table I. Figures S3 and S4 of the supplementary material report the fluorescence polarization experiments performed for the determination of the phase transition temperatures, T_c, for vesicles made of pure **1** and **2** and of the blends with nonfunctional surfactants **5** and **6**.

Table I. Physical Properties of the Aggregates Made from Different Surfactants in 0.05 M MES Buffer (pH 6.3)

surfactant	aggregate	10^5(cmc), M	diameter, Å	T_c, °C
1	vesicles	<0.1	650 ± 250[a]	15 (16)[b]
2	vesicles	<0.1	550 ± 200[a]	39.5 (34)[b]
3	micelles	1.5	n.d.	

[a] From the Gaussian analysis of the light scattering data. Using the more sophisticated NICOMP ILT algorithm (Nicomp Particle Sizing Systems, Santa Barbara, CA), bimodal distributions are apparent with hydrodynamic diameters of ~200 and ~900 Å for **1**, ~300 and ~1,100 Å for **2**. This latter population becomes even less important upon addition of Cu(II) ions. [b] In the presence of $[Cu(NO_3)_2] = 1.8 \times 10^{-4}$ M.

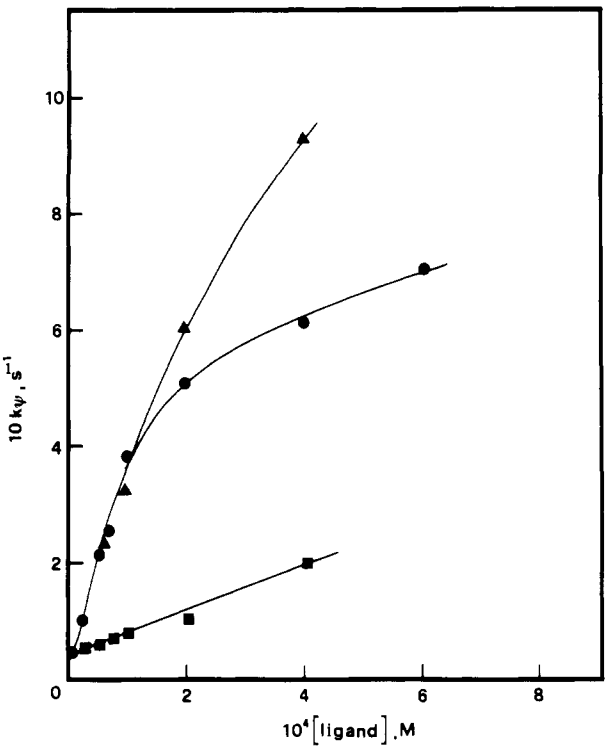

Figure 1. Rate vs concentration profiles for the cleavage of PNPP at different ligand concentrations in homoaggregates. Conditions: 0.05 M MES buffer (pH 6.3), 25 °C, $[Cu^{2+}] = 1.8 \times 10^{-4}$ M. ▲, ligand **1**; ■, ligand **2**; ●, ligand **3**.

(9) (a) Fornasier, R.; Scrimin, P.; Tecilla, P.; Tonellato, U. *J. Am. Chem. Soc.* **1989**, *111*, 224. (b) Scrimin, P.; Tecilla, P.; Tonellato, U. *J. Org. Chem.* **1991**, *56*, 161. (c) Fornasier, R.; Scrimin, P.; Tonellato, U.; Zanta, N. *J. Chem. Soc., Chem. Commun.* **1988**, 716. (d) Fornasier, R.; Milani, D.; Scrimin, P.; Tonellato, U. *J. Chem. Soc., Perkin Trans. 2* **1986**, 233.

(10) Hydrolytic metallovesicles of very low solubility have been reported by Menger: Menger, F. M.; Gan, L. H.; Johnson, E.; Durst, D. H. *J. Am. Chem. Soc.* **1987**, *109*, 2800. For an example of the interaction of Cu^{2+} with nucleophilic vesicles, see ref 5c. Chelating vesicles: Fuhrhop, J.-H.; Koesling, V.; Schoenberger, G. *Liebigs Ann. Chem.* **1984**, 1634. van Esch, J. H.; Stols, A. L. H.; Nolte, R. J. M. *J. Chem. Soc., Chem. Commun.* **1990**, 1658.

(11) Fife, T. H.; Przystas, T. J. *J. Am. Chem. Soc.* **1985**, *107*, 1041 and references therein.

(12) Fornasier, R.; Milani, D.; Scrimin, P.; Tonellato, U. *Gazz. Chim. Ital.* **1986**, *116*, 55.

(13) Amundsen, A. R.; Whelan, J.; Bosnich, B. *J. Am. Chem. Soc.* **1977**, *99*, 6730.

(14) Szoka, F.; Papahadjopoulos, D. *Annu. Rev. Biophys. Bioeng.* **1980**, *9*, 467. Lasic, D. L. *Biochem. J.* **1988**, *256*, 1.

(15) It is known that EB does not permeate cationic vesicles: Moss, R. A.; Swarup, S.; Wilk, B.; Hendrickson, T. *Tetrahedron Lett.* **1985**, *26*, 4827.

Scheme II

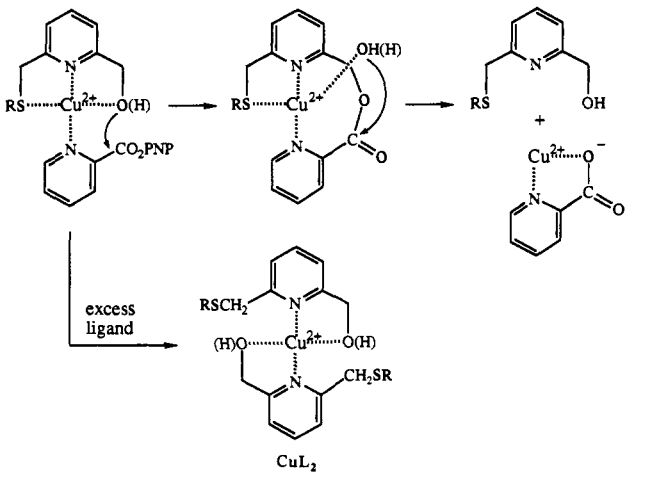

The binding constant for the 1:1 complex with Cu^{2+} in methanol (where no aggregates are formed) is ca. $10^{4.7}$ for all ligands[16] and decreases 1 order of magnitude in water in the presence of the aggregates: no significant differences related either to the structure of the surfactant or the nature of the molecular assembly were observed.

Cleavage of PNPP: Kinetic Studies. In Figure 1 we have reported the rate vs concentration profiles for the hydrolysis of PNPP in the presence of a fixed amount of Cu^{2+} ($[Cu^{2+}] = 1.8 \times 10^{-4}$ M) for the three surfactants studied. Kinetics were run under pseudo-first-order conditions (see Experimental Section for details) following the appearance of *p*-nitrophenoxide at 400 nm. The pH chosen, 6.3, is the highest value experimentally accessible to ensure stable Cu^{2+} solutions and maximum kinetic effects. It must be pointed out that at the surface of the cationic aggregates the effective pH is slightly higher due to the presence of OH^- as a counterion. In the typical experimental protocol, the aggregates were created in the buffer solution *before* the addition of the $Cu(NO_3)_2$ solution and the kinetics started upon the addition of the substrate. No changes in the rate constant and final absorbance were apparent when the vesicles were created in the presence of PNPP and the kinetics initiated by the addition of Cu^{2+}. On the other hand, experiments with vesicles obtained in the presence of Cu^{2+} could not be performed, as sonication resulted in extensive decomposition[17] of the surfactant. The two vesicular aggregates present quite different behavior: the one made of the "natural backbone" surfactant, **2**, is a rather modest catalyst ($k_\psi/k_o = 5.0$ being [**2**] $= 4 \times 10^{-4}$ M and $[Cu^{2+}] = 1.8 \times 10^{-4}$ M; k_o is the observed rate constant of the Cu^{2+}-catalyzed process), while that containing the dialkylammonium amphiphile, **1**, proves to be a more effective system ($k_\psi/k_o = 20.5$, same conditions as for **2**; see above). The rate profile obtained in the case of micelles made of surfactant **3** is similar to that of vesicular **1** up to a concentration close to that of the metal ion and reaches a limiting value at a ligand concentration larger than that of Cu^{2+}.

We have previously shown[9a] that the critical feature for the occurrence of the catalytic process in analogous micellar systems is the formation of a ternary complex involving surfactant ligand, metal ion, and substrate (Scheme II). In the presence of excess surfactant over metal ion, the formation of *nonproductive* ternary complexes (two ligand molecules for a single Cu^{2+} ion, L_2Cu, where L indicates the ligand) leads to the depression of the kinetic effects.[9a,b]

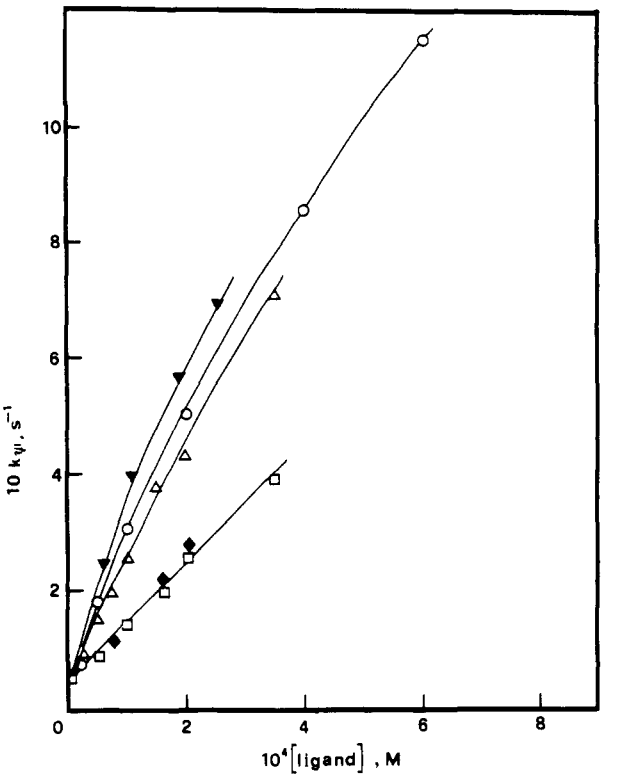

Figure 2. Rate vs concentration profiles for the cleavage of PNPP in coaggregates. Conditions: 0.05 M MES buffer (pH 6.3), 25 °C, $[Cu^{2+}] = 1.8 \times 10^{-4}$ M, [additive] = 10[ligand] in all cases. ○, comicelles made of **3** and CTABr; ▼, covesicles made of **1** and **5**; △, covesicles made of **1** and **6**; □, covesicles made of **2** and **6**; ♦, covesicles made of **2** and **5**.

On the basis of these arguments, we attributed the behavior of micellar surfactant **3** to the formation of these nonproductive complexes in the presence of excess surfactant over Cu^{2+}. Assuming that this effect is the only factor responsible for the modification of the reactivity, one is forced to conclude that the formation of kinetically nonproductive L_2Cu complexes is not important in the case of vesicular **1** and, on the contrary, quite relevant in that of vesicular **2**.

In order to check this point, we ran our kinetic experiments using solutions in which the different surfactants were dispersed in a matrix made of an "inert" amphiphile featuring the same lipophilic moiety, namely, surfactants **5**, **6**, and *n*-hexadecyltrimethylammonium bromide (CTABr) for **1**, **2**, and **3**, respectively. Under these conditions, we expected to break down the formation of the L_2Cu complexes and enhance the catalytic efficiency of systems **2** and **3**.

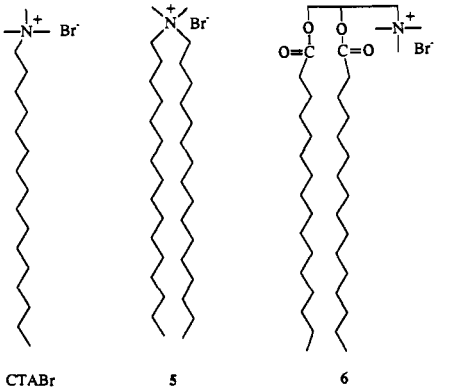

CTABr 5 6

The data reported in Figure 2 show that our expectation was fulfilled in the case of micellar **3** also under conditions [**3**] > $[Cu^{2+}]$, while for vesicular **2**, though some increase in reactivity was observed, the kinetic effect still remained *roughly one-half* that of the other two systems. Therefore, other phenomena are likely to govern the reactivity of this latter vesicular system.

(16) Scrimin, P.; Tecilla, P.; Tonellato, U.; Vendrame, T. *J. Org. Chem.* **1989**, *54*, 5988. The binding constant for Cu^{2+} of vesicles made of surfactant **1** (not reported in this reference) is close to this value. It could be determined only with some uncertainty due to the instability (turbidity develops within 1–2 min) of these aggregates in the presence of the relatively high Cu^{2+} concentration used for binding constant determination.

(17) Analysis of the decomposition products shows oxidative cleavage of the C–S bond with formation, among other products, of a 2-formylpyridino derivative. In spite of several attempts to perform sonication in an atmosphere devoid of oxygen, we were unable to control this decomposition process.

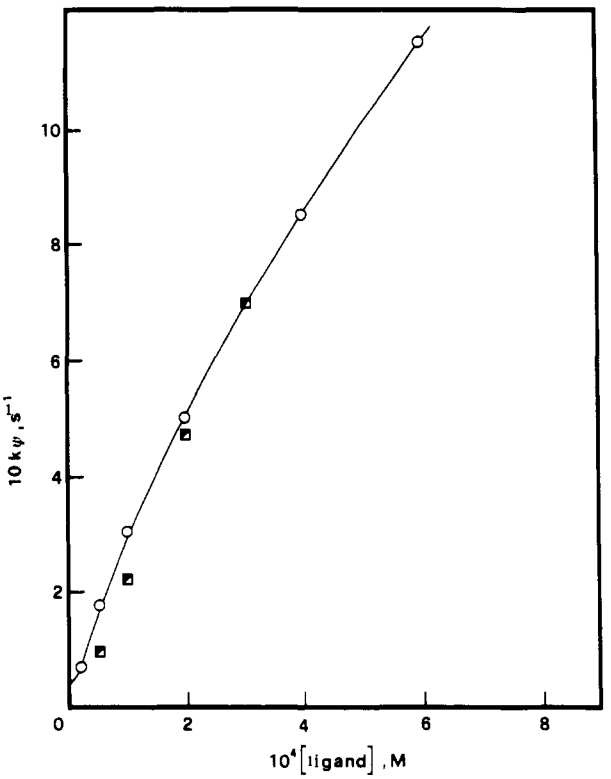

Figure 3. Rate vs concentration profiles for the cleavage of PNPP at different ligand concentrations for 3 (○) and 2 (◪) comicellized with CTABr. Conditions as in Figure 2.

Furthermore, kinetic data reported in the same Figure 2 show that the catalytic effect is *not dependent* on the nature of the vesicular matrix in which ligand **1** or **2** is dispersed. Within the limit of the experimental error, the same reactivity was observed in the case of ligand **1** when covesicallized with either **5** and **6**, whereas ligand **2** presents half the kinetic efficiency of **1** in either vesicular **5** or vesicular **6**. In order to rule out any dependence of the reactivity on the structure of ligand **2**, we performed kinetic experiments with this surfactant comicellized with CTABr. Under these conditions (Figure 3), its reactivity is similar to that of micellar **3**. Accordingly, the different reactivity of **2** *must be ascribed to the structure of the vesicular aggregates.*

Cu^{2+} Binding: Spectroscopic and Kinetic Measurements. The thioether sulfur present at the binding site of ligands **1–3** allows the observation of an absorption band, upon complexation with Cu^{2+}, in the 310–330-nm region. This band is due to a $S(\sigma) \rightarrow Cu(d_{x^2-y^2})$ transition and has been well characterized for other thioether donors by Bosnich and his co-workers.[13] It makes possible the easy monitoring[16] of the amount of complex formed in the presence of the aggregates made of ligands **1–3**. As mentioned before, in the case of vesicular **1** and **2**, the binding constant is rather similar for the two aggregates, as is their molar extinction coefficient (ϵ 2300 ± 100), and therefore, the observed absorbance may give information on the permeability of the Cu^{2+} ions across the vesicular membranes. Since Cu^{2+} is added *after* creation of the vesicles, if permeation *does occur*, all the ligands (internal and external layer) are involved in the complex formation, while if permeation *does not occur*, only the ligands of the external layer of the aggregate can form the complexes. Table II reports the absorbances measured at the wavelength of the maxima for the different complexes. Analysis of Table II reveals that micellar **3** and vesicular **1** present similar absorbances. On the contrary, in the case of vesicular **2**, only ca. *half* the absorbance observed for the other two aggregates is measured.

These data are strongly supported by stopped-flow experiments which allowed us to monitor the kinetics of Cu^{2+} binding to the different aggregates. A typical experiment is reported in Figure 4. It shows how in the case of micellar **3** and vesicular **2** a single monotonic[18] increase of absorbance is observed, leading, in the case of **2**, to roughly *half the final absorbance observed for 3.*[19] On the other hand, with vesicular **1**, the first fast increase of absorbance (amounting again to half the total absorbance—the two ΔA's ranged from 52:48 to 60:40 in different runs—observed for **3**) is followed by a slower process. This latter slow kinetic is of the same order of magnitude as the rate observed, under identical conditions, for the cleavage of PNPP. Analogous experiments with covesicles could not be performed due to a too small change in absorbance with these systems. Thus, by all evidence, the two vesicular systems differ quite remarkably in Cu^{2+} ion permeation across the membrane: vesicles made of ligand **2** appear impermeable to the metal cations, while those made of **1** appear permeable in a rather fast process. Micelles of **3** obviously do not present permeation problems.

Table II. Absorbances of the Different Aggregates in the Presence of Cu^{2+} in 0.05 M MES Buffer (pH 5.5)[a] at 25 °C[b]

ligand	λ_{max}, nm	aggregate	A
1	322	vesicles	0.32[c]
2	318	vesicles	0.19
3	321	micelles	0.36

[a] At higher pH, some Cu^{2+} precipitation occurs due to the relatively high concentration used in the experiment. [b] [Ligand] = 3.3×10^{-4} M; $[Cu^{2+}] = 1.4 \times 10^{-3}$ M. [c] Determined with some uncertainty (see ref 16). This value is the average of three readings.

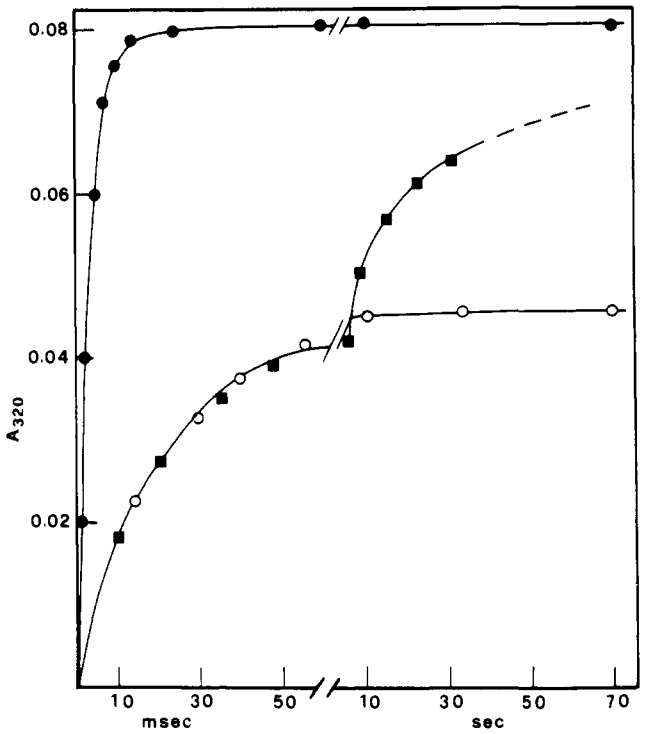

Figure 4. Observed change of absorbance vs time upon addition of $Cu(NO_3)_2$ to different aggregates. Conditions: 0.05 M MES buffer (pH 5.5), 25 °C, [surfactant] = 5×10^{-4} M, $[Cu^{2+}] = 3.3 \times 10^{-4}$ M. Note the change in the time scale. ■, vesicular **1**; ○, vesicular **2**; ●, micellar **3**. (Final absorbance for **1** could not be recorded due to the formation of some turbidity after ca. 60 s.)

Reactivity in Metallomicelles and Metallovesicles. The above kinetic and spectroscopic data are consistent with the idea that two major phenomena regulate the reactivity of the present ligand

(18) The rate of binding of Cu^{2+} to aggregates appears quite slow as compared to "monomeric" ligands. This is the object of a parallel investigation; see: Tondre, C.; Claude-Montigny, B.; Ismael, M.; Scrimin, P.; Tecilla, P. *Polyhedron* **1991**, *10*, 1791.

(19) After this fast kinetic process, a slow increase of absorbance is observed for vesicular **2**, which could be analyzed as a pseudo-first-order process ($k_\psi \sim 1 \times 10^{-4}$ s^{-1}). Careful control of the system allowed us to attribute this increase of absorbance to the oxidative cleavage of the ligand subunit (see ref 17) rather than to Cu^{2+} permeation. Accordingly, this latter must occur with a rate constant similar to or slower than that of decomposition.

vesicles: (i) formation of productive and nonproductive complexes; (ii) permeability of the membranes to Cu^{2+} ions.

The formation of nonproductive ternary complexes (L_2Cu; see Scheme II) appears to be controlled by the ligand/Cu^{2+} ratio in homomicelles where the ligand surfactants aggregate in a disordered way and are not forced to assume any specific geometry. Vesicles present a more ordered aggregation mode not only in the gel phase, below the T_c, but also above it, as the kinking of the hydrocarbon chain occurring above the T_c is known[20] to involve preferentially the very last C–C bonds. Thus, the ability to form nonproductive complexes appears related, in these cases, to the mobility of the parts of the molecules oriented toward the bulk water solution. Inspection of CPK molecular models indicates more degrees of freedom for the pyridine subunit of **2** when compared to that of **1** because it is further removed from the surface of the membrane (i.e., the atom from which the two hydrocarbon chains originate). Therefore, we suggest that in the case of **1** the ligand moiety of the molecules is somehow forced to stick out the surface of the vesicles and cannot easily form ternary complexes within the very same aggregate. On the other hand, in the case of **2** this is not only geometrically easier but also highly favored by the fact that the surfactant is constrained in the vesicular membrane. Indirect support to this suggestion comes from the observation that vesicles made of **1** are rather unstable (see ref 16) in the presence of Cu^{2+} and tend to fuse and eventually precipitate, while those made of surfactant **2** are more stable. Fusion could be due to the formation of intervesicular ternary complexes. A similar process has been suggested to be responsible of fusion of anionic or zwitterionic vesicles in the presence of divalent cations.[21]

However, these observations provide, only in part, a rationale to the reactivity data reported in Figure 1 and, particularly, to the different behavior of the two vesicular systems. Another issue must be taken into account: the permeation of the different species (Cu^{2+}, PNPP) across the vesicular membrane. In order to explain the kinetic and spectroscopic data as well, we offer the following suggestion. (a) Neutral PNPP freely crosses the bilayer at a rate faster than the hydrolytic process studied.[22] In fact, no changes in the rate constants and amount of *p*-nitrophenol released have been observed on changing the order of PNPP addition (before or after vesicle creation). (b) Neither cationic vesicle allows *passive* transport of Cu^{2+} cations across the membrane: as a matter of fact, the kinetic effects shown in Figure 2 are *not* dependent on the nature of the vesicular membrane in which the ligand surfactants are embedded. (c) Cu^{2+} cation permeation is the result of the transport by the ligand surfactants as Cu(II) complexes. We suggest that this transport is regulated by *the rate of flip-flop of 1 and 2* and is not related to the phase transition temperature[23] (15 °C in the case of the dialkylammonium surfactant) because, in the covesicallized systems, T_c is similar to that of the nonfunctional matrix (26 and 28.5 °C for **1** + **5** and **2** + **5**, respectively, 37 °C for **1** + **6**, and 37.5 °C for **2** + **6**; see Figures S3 and S4 of the supplementary material) and not to that of the functional additive. The scarce relevance of T_c on the observed phenomena is confirmed by the Arrhenius plots measured for aggregates made of **1**–**3** (see Figure S5 of the supplementary material). Though some increase of the kinetic efficiency is observed for both **1** and **2** above T_c, this does not account for the difference in reactivity between the two systems. As an alternative explanation, there may be some sorting of the mixed aggregates in domains where **1** or **2** cluster and thus control vesicle permeability as in homovesicles. The formations of domains in covesicles has been reported by Kunitake and his associates,[5c] and it appears to be also triggered by the addition of Cu(II) ions. These authors found that domains survive up to a 1:20 dilution in a nonfunctional matrix and then collapse abruptly. In our case, the reactivity of mixed aggregates changes in a monotonic way by varying the functional/nonfunctional aggregate ratio for all systems (see Figure S6 of the supplementary material).[24] Such an observation does not favor the hypothesis of the formation of domains more extended than the L_2Cu complexes mentioned above.

In conclusion, the kinetic and spectroscopic data suggest fast Cu^{2+} transport in the case of **1** and very slow (or negligible) transport in the case of **2**. Within the limit of the time scale of our kinetic experiments, the rate of transport seems not to be dependent on the nature of the inert surfactant used for covesicallization. The flip-flop suggestion is supported by recent data by Moss and his co-workers:[8] they observed (at 25 °C) very fast flip-flop for dihexadecylmethylammonium surfactants (like **1**) in contrast with a rather slow one for cationic surfactants featuring a glyceryl diester backbone (like **2**).[8b] However, in the Moss system the nature of the matrix *does* control the flip-flop rate[25] so that a functional surfactant made of a glycerol like backbone shows a much faster flip-flop rate when embedded in a dihexadecylammonium matrix. This appears not to be the case with surfactant **2**, though it should be emphasized that we are dealing with a Cu^{2+}-bound cationic surfactant, i.e., a highly charged species. The effect of headgroups on transbilayer movements is largely unexplored, and further investigation is obviously needed.

We plan, in the near future, to confirm this interpretation and finely tune the transbilayer movements governing the permeation of Cu^{2+} (and other) ions in order to control reactivity and, perhaps, electron transfer[26] in artificial liposomes. The final goal is the design of totally artificial molecular devices able to rival the selectivity observed in the case of biological membranes.

Experimental Section

General Methods. Melting points are uncorrected. ^1H NMR spectra were recorded on a 200-MHz Bruker WP-200 SY spectrometer, and chemical shifts in ppm are reported relative to internal Me_4Si. UV–Vis spectra were recorded on a Perkin-Elmer Lambda 5 spectrophotometer equipped with a thermostated cell holder. Fluorescence spectra were recorded on a Perkin-Elmer MPF-66 spectrofluorimeter. Surface tension measurements to evaluate the critical micelle concentration (cmc) of the micellar solution were made on a Krüss Type 8451 tensiometer. Vesicle sizes were determined by dynamic light scattering using a Nicomp 370 autocorrelator equipped with a Spectra-Physics 2016 argon laser. Microanalyses were performed by the Laboratorio di Microanalisi of this Department.

Materials. The diethyl ester of chelidamic acid was synthesized from chelidamic acid (Janssen) as described.[16] $Cu(NO_3)_2$ was an analytical grade commercial product. The Cu^{2+} stock solution was titrated against EDTA as previously reported.[9a] PNPP was prepared and purified by literature methods.[9a] 2-(*N*-Morpholino)ethanesulfonic acid (MES), used as the buffer, was a Fluka product, used as received. *n*-Hexadecyltrimethylammonium bromide (CTABr) was an analytical grade commercial product. Di(*n*-hexadecyl)dimethylammonium bromide[27] (**5**) and 1,2-bis(palmitoyloxy)-3-(trimethylammonio)propane[7b] (**6**) were prepared as reported.

4-[(2-Bromoethyl)oxy]-2-(hydroxymethyl)-6-[(methylthio)methyl]-pyridine (4). To a stirred solution of chelidamic acid diethyl ester (1.0 g, 4.2 mmol) in 25 mL of EtOH was added $NaBH_4$ (0.790 g, 20 mmol). After H_2 evolution ceased, finely powdered $CaCl_2$ (2.32 g, 20 mmol) was added in small portions. The slurry was vigorously stirred for 2 h at room temperature. Excess hydride was then quenched with water and the resulting suspension evaporated to dryness. The white gummy material obtained was suspended in 50 mL of $SOCl_2$ and stirred at room tem-

(20) Lee, A. G. *Prog. Biophys. Molec. Biol.* **1975**, *29*, 3.
(21) See ref 1, pp 148–149.
(22) Fast permeation of small neutral molecules across liposomal membranes has been reported: see ref 1, p 151.
(23) It is known that at or above T_c permeation phenomena may become faster because the membrane bilayer gets less ordered and more fluid. See, for instance, ref 15 and: Moss, R. A.; Hendrickson, T. F.; Swarup, S.; Hui, Y.; Marky, L.; Breslauer, K. J. *Tetrahedron Lett.* **1984**, *25*, 4063.
(24) These rate profiles show an increase of k_ψ for vesicular **2** as the [6]/[2] ratio increases; an increase of k_ψ is also observed for micellar **3** followed, at very high [CTABr]/[3] ratios, by a slight decrease. While the increase reflects, in both cases, the breakdown of L_2Cu complexes, the decrease, in the case of **3**, is likely to be due to the "dilution" of the active surfactant in the micellar matrix, thus decreasing the amount of productive ternary complexes, as it is commonly found in comicelles made of mixtures of functional/nonfunctional surfactants. The latter explanation may be offered for the rate decrease observed with vesicular **1** as the ratio [5]/[1] increases and is in line with the assumption (see text) that L_2Cu complexes are not formed within these vesicles.
(25) Moss, R. A. Private communication to P.S., May 1990.
(26) Robinson, J. N.; Cole-Hamilton, D. J. *Chem. Soc. Rev.* **1991**, *20*, 49.
(27) Ueoka, R.; Matsumoto, Y. *J. Org. Chem.* **1984**, *49*, 3774.

perature for 6 h, protected from moisture ($CaCl_2$). Evaporation of the $SOCl_2$ afforded a white powder, which was suspended in toluene, and the solvent was removed to eliminate residues of the chlorinating agent. The white solid obtained (0.870 g, 82%), mp 159.5–161.5 °C, was the HCl salt of ethyl 6-(chloromethyl)-4-hydroxy-2-pyridinecarboxylate: ^{1}H NMR δ (1:1 $CDCl_3/CD_3OD$) 1.41 (t, J = 7.2 Hz, 3 H, CH_2CH_3); 4.39 (q, J = 7.2 Hz, 2 H, CH_2CH_3); 4.60 (s, 2 H, $ClCH_2Py$); 6.97 and 7.30 (2 d, J = 2.2 Hz, 2 H, Py H_3 and H_5).

To the above chloride (1.97 g, 9.1 mmol) dissolved in 100 mL of dry EtOH was added $NaSCH_3$ (1.28 g, 18 mmol), and the resulting solution was heated at reflux for 30 min, under a nitrogen atmosphere. After the solution cooled at room temperature, a white precipitate was filtered off and washed with EtOH. The combined organic washings were evaporated to give a crude that was treated with water and extracted with $CHCl_3$ (3 × 100 mL). The dried organic layer (Na_2SO_4) was evaporated under reduced pressure to leave 2.10 g (94%) of ethyl 4-hydroxy-6-[(methylthio)methyl]-2-pyridinecarboxylate as a pale yellow oil: ^{1}H NMR δ ($CDCl_3$) 1.39 (t, J = 7.2 Hz, 3 H, CH_2CH_3); 2.03 (s, 3 H, SCH_3); 3.68 (s, 2 H, SCH_2Py); 4.40 (q, J = 7.2 Hz, 2 H, CH_2CH_3); 6.62 and 7.17 (2 d, J = 2.4 Hz, 2 H, Py H_3 and H_5).

To a solution of the previous material (2.55 g, 11 mmol) in 100 mL of EtOH was added $NaBH_4$ (0.850 g, 22 mmol). After H_2 evolution ceased, finely powdered $CaCl_2$ (2.49 g, 22 mmol) was added in small portions. After the solution was stirred vigorously for 1 h, 100 mL of water was added to the reaction mixture. The EtOH was evaporated at reduced pressure, and the pH of the remaining aqueous solution was adjusted to 6 with concentrated HCl. This solution was continuously extracted with $CHCl_3$ for 3 weeks to give 1.45 g (70%) of (white solid) 2-(hydroxymethyl)-4-hydroxy-6-[(methylthio)methyl]pyridine: ^{1}H NMR δ (CD_3OD) 2.05 (s, 3 H, SCH_3); 3.64 (s, 2 H, SCH_2Py); 4.53 (s, 2 H, OCH_2Py); 6.32 and 6.40 (2 d, J = 2.44 Hz, 2 H, Py H_3 and H_5).

This thioether derivative (0.40 g, 2.2 mmol) was added to a DMF solution containing 5 mL of 1,2-dibromoethane and 18-crown-6 (0.66 g, 2.5 mmol). Finely powdered K_2CO_3 (0.59 g, 4.4 mmol) was then added, and the vigorously stirred slurry was kept at 80 °C for 8 h. The DMF was then distilled at reduced pressure and the remaining crude material treated with water and extracted with $CHCl_3$ (3 × 100 mL). The combined organic layers were dried over Na_2SO_4 and evaporated to afford 0.59 g (93%) of **4**: ^{1}H NMR δ ($CDCl_3$) 2.08 (s, 3 H, SCH_3); 3.65 (t, J = 6.9 Hz, 2 H, OCH_2CH_2Br); 3.75 (s, 2 H, SCH_2Py); 4.35 (t, J = 6.9 Hz, 2 H, OCH_2CH_2Br); 4.60 (s, 2 H, OCH_2Py); 6.63 and 6.81 (2 d, J = 2.4 Hz, 2 H, Py H_3 and H_5).

4-[[2-(*n*-Hexadecyldimethylammonio)ethyl]oxy]-2-(hydroxymethyl)-6-[(methylthio)methyl]pyridine Bromide (3). A solution of **4** (0.193 g, 0.66 mmol) and *n*-hexadecyldimethylamine[28] (0.195 g, 0.72 mmol) in 20 mL of CH_3CN was heated in an oil bath at 80 °C for 48 h. The solvent was then evaporated at reduced pressure and the crude material obtained chromatographed on neutral alumina ($CHCl_3$/MeOH from 9:1 to 8:2) to afford 0.270 g (73%) of **3**, which was crystallized from acetone/ethyl ether, mp 103–105 °C: ^{1}H NMR δ (CD_3OD) 0.941 (br t, J = 6.71 Hz, 3 H, $(CH_2)_{15}CH_3$); 1.41 (m, 26 H, $(CH_2)_{13}CH_3$); 1.89 (m, 2 H, $(CH_2)_nCH_2CH_2N$); 2.08 (s, 3 H, SCH_3); 3.26 (s, 6 H, $N(CH_3)_2$); 3.49 (m, 2 H, $NCH_2(CH_2)_n$); 3.78 (s, 2 H, SCH_2Py); 3.92 (m, 2 H, NCH_2CH_2O); 4.66 (m, 2 H, NCH_2CH_2O); 4.69 (s, 2 H, OCH_2Py); 7.03 and 7.12 (2 d, J = 2.44 Hz, 2 H, Py H_3 and H5).

Anal. Calcd for $C_{28}H_{53}N_2O_2SBr$: C, 59.88; H, 9.51; N, 4.98. Found: C, 59.47; H, 9.60; N, 4.85.

4-[[2-[Di(*n*-hexadecyl)methylammonio]ethyl]oxy]-2-(hydroxymethyl)-6-[(methylthio)methyl]pyridine Bromide (1). To a solution of *n*-hexadecylamine (3.0 g, 12 mmol) in 100 mL of toluene was added 1.32 g of benzaldehyde (12 mmol). This solution was heated at reflux for 2 h and the water formed during the reaction removed by means of a Dean-Stark trap. After the solution cooled at room temperature, the organic solvent was distilled under reduced pressure, leaving quantitatively the imine derivative: ^{1}H NMR δ ($CDCl_3$) 0.89 (br t, 3 H, $(CH_2)_nCH_3$); 1.30 (m, 26 H, $(CH_2)_{13}CH_3$); 1.71 (m, 2 H, $NCH_2CH_2(CH_2)_n$); 3.64 (br t, 2 H, $NCH_2(CH_2)_n$); 7.47 (m, 3 H, Ph H_{3-5}); 7.72 (m, 2 H, Ph H_2 and H_6); 8.27 (br s, 1 H, CH=N). This material (4.02 g, 12 mmol) dissolved in 100 mL of CH_2Cl_2 was poured in a screw-top pressure tube and cooled to −78 °C. After the addition of 3.3 mL of CH_3Br (60 mmol), the tube was sealed and kept at 70 °C in an oil bath for 48 h. The solvent was then evaporated and the residue treated with 100 mL of 0.1 M NaOH and extracted with $CHCl_3$. The evaporation of the dried organic layer (Na_2SO_4) afforded a crude material that was purified by dissolving it in acetone and precipitating the HCl salt of the amine upon addition of concentrated HCl. The white solid *n*-hexadecylmethylamine hydrochloride, 3.18 g (91%), was collected and washed several times with acetone, mp 176–177 °C (lit.[28] 178 °C): ^{1}H NMR δ (CD_3OD) 0.90 (br t, 3 H, $(CH_2)_nCH_3$); 1.34 (m, 26 H, $(CH_2)_{13}CH_3$); 1.66 (m, 2 H, $NCH_2CH_2(CH_2)_n$); 2.69 (s, 3 H, NCH_3); 2.98 (m, 2 H, $NCH_2(CH_2)_n$).

Of the above amine hydrochloride, 0.21 g was dissolved in 100 mL of $CHCl_3$ and washed once with a saturated solution of $NaHCO_3$ and then twice with deionized water. The evaporation of the dried organic solvent (Na_2SO_4) afforded 0.18 g (0.71 mmol) of *n*-hexadecylmethylamine that was dissolved in 20 mL of MeCN. To this solution, placed in a screw-top pressure tube were added **4** (0.19 g, 0.65 mmol) and 0.35 mL of diisopropylethylamine (2.0 mmol). The tube was then sealed and kept at 80 °C in an oil bath for 12 h. After evaporation of the solvent, the crude material obtained was purified by chromatography (SiO_2, $CHCl_3$/MeOH 20:1) to give 0.225 g (62%) of pure 4-[[2-(*n*-hexadecylmethylamino)-ethyl]oxy]-2-(hydroxymethyl)-6-[(methylthio)methyl]pyridine hydrobromide, as a white solid: ^{1}H NMR δ (10:1 $CDCl_3$:CD_3OD) 0.88 (br t, 3 H, $(CH_2)_nCH_3$); 1.31 (m, 26 H, $(CH_2)_{13}CH_3$); 1.73 (m, 2 H, $NCH_2CH_2(CH_2)_n$); 2.07 (s, 3 H, SCH_3); 2.75 (br s, 3 H, NCH_3); 2.95 (m, 2 H, $NCH_2(CH_2)_n$); 3.41 (m, 2 H, NCH_2CH_2O); 3.73 (s, 2 H, SCH_2Py); 4.50 (m, 2 H, NCH_2CH_2O); 4.67 (s, 2 H, OCH_2Py); 6.84 and 6.92 (2 d, J = 2.14 Hz, 2 H, Py H_3 and H_5).

The previous material was converted into the free amine (0.190 g, 0.4 mmol) by treating it with $NaHCO_3$ and was dissolved in a 1:1 mixture of EtOH and MeCN. After addition of 0.621 g (2.0 mmol) of *n*-hexadecyl bromide (Aldrich), the reaction mixture, sealed in a screw-top pressure tube, was heated at 80 °C in an oil bath for 36 h. The solvent was removed under reduced pressure and the crude material obtained purified by chromatography (neutral alumina, $CHCl_3$/MeOH 15:1) to give a gummy material. This was crystallized from acetone/pentane to afford 0.200 g (64%) of **1**, mp ≈75 °C (gel), ≈140 °C (liquid crystal): ^{1}H NMR δ (CD_3OD) 0.94 (br t, 6 H, $(CH_2)_nCH_3$); 1.33 (m, 52 H, $(CH_2)_{13}CH_3$); 1.85 (m, 4 H, $NCH_2CH_2(CH_2)_n$); 2.08 (s, 3 H, SCH_3); 3.20 (s, 3 H, NCH_3); 3.46 (m, 4 H, $NCH_2(CH_2)_n$); 3.78 (s, 2 H, SCH_2Py); 3.91 (m, 2 H, NCH_2CH_2O); 4.62 (m, 2 H, NCH_2CH_2O); 4.69 (s, 2 H, OCH_2Py); 7.01 and 7.11 (2 d, J = 2.4 Hz, 2 H,Py H_3 and H_5).

Anal. Calcd for $C_{43}H_{83}N_2O_2SBr$: C, 66.89, H, 10.84; N, 3.63. Found: C, 66.49; H, 10.92; N, 3.59.

4-[[2-[[1,2-Bis(palmitoyloxy)-3-propyl]dimethylammonio]ethyl]oxy]-2-(hydroxymethyl)-6-[(methylthio)methyl]pyridine Bromide (2). 3-Bromo-1,2-propanediol (Fluka, 1.5 g, 9.7 mmol) dissolved in 50 mL of MeOH was poured in a screw-top pressure tube and cooled to 0 °C in an ice bath. After addition of 6 mL of dry dimethylamine (Fluka) to this cooled solution, the tube was sealed and kept under stirring at room temperature for 2 days. The solvent was then distilled at reduced pressure to give in almost quantitative yield the 3-(dimethylamino)-1,2-propanediol hydrobromide. The free amine was obtained by treating the above salt with a stochiometric amount of sodium ethoxide in EtOH. A white precipitate was filtered off and the EtOH evaporated to afford 1.09 g (95%) of pure 3-(dimethylamino)-1,2-propanediol as a pale yellow oil: ^{1}H NMR δ (CD_3OD) 2.27 (s, 6 H, $N(CH_3)_2$); 2.40 (m, 2 H, CH_2CHCH_2N); 3.49 (m, 2 H, CH_2CHCH_2N); 3.77 (m, 1 H, CH_2CHCH_2N).

To a solution of **4** (0.50 g, 1.7 mmol) in 25 mL of CH_2Cl_2 were added 1.5 mL of 3,4-dihydro-2*H*-pyran and 0.212 g (0.8 mmol) of pyridinium *p*-toluenesulfonate.[29] This solution protected from moisture ($CaCl_2$), was stirred at room temperature for 12 h. Thereafter, CH_2Cl_2 (100 mL) was added and the organic solvent washed 3 times with water. The dried organic layer (Na_2SO_4) was evaporated at reduced pressure and the crude material thus obtained chromatographed over silica ($CHCl_3$) to afford 0.54 g (84%) of 4-[(2-bromoethyl)oxy]-2-[[(tetrahydro-2-pyranyl)oxy]methyl]-6-[(methylthio)methyl]pyridine: ^{1}H NMR δ (CD_3OD) 1.43–2.01 (m, 6 H, THP); 2.03 (s, 3 H, SCH_3); 3.54 (m, 1 H, THP H_6); 3.72 (s, 2 H, SCH_2Py); 3.75 (m, 2 H, OCH_2CH_2Br); 3.90 (m, 1 H, THP H_6); 4.43 (m, 2 H, OCH_2CH_2Br); 4.55 and 4.76 (AB, J = 13.8 Hz, 2 H, OCH_2Py); 4.76 (m, 1 H, THP H_2); 6.95 and 6.99 (2 d, J = 2.12 Hz, 2 H, Py H_3 and H_5).

To a solution of the above bromide (0.402 g, 1.1 mmol) in 30 mL of CH_3CN was added 3-(dimethylamino)-1,2-propanediol (0.254 g, 2.1 mmol). After the solution was heated for 2 days at 80 °C in an oil bath, the solvent was stripped to leave a crude oil that was dissolved in a little MeOH and then precipitated with ethyl ether. The organic solvent was decanted and discarded. The remaining clear oil was dried in vacuo to give 0.450 g (85%) of 4-[[2-[[1,2-dihydroxy-3-propyl]dimethylammonio]ethyl]oxy]-2-[[(tetrahydro-2-pyranyl)oxy]methyl]-6-[(methylthio)methyl]pyridine bromide: ^{1}H NMR δ (CD_3OD) 1.55–2.18 (m, 6 H, THP); 2.25 (s, 3 H, SCH_3); 3.32 (s, 6 H, $N(CH_3)_2$); 3.62–3.88 (m, 5 H, THP H_6, $NCH_2CH(OH)CH_2(OH)$); 3.95 (s, 2 H, SCH_2Py); 4.10 (m, 1 H, THP H_6); 4.22 (br t, 2 H, NCH_2CH_2O); 4.44 (m, 1 H,

(28) Westphal, O.; Jerchel, D. *Chem. Ber.* **1940**, *73*, 1002.

(29) Miyashita, M.; Yoshikoshi, M.; Grieco, P. A. *J. Org. Chem.* **1977**, *42*, 3772.

$CH_2CH(OH)CH_2(OH)$); 4.72–5.07 (m, 5 H, THP H_2, NCH_2CH_2O, and OCH_2Py); 7.25 (m, 2 H, Py H_3 and H_5).

To the previous diol (0.37 g, 0.75 mmol) dissolved in 50 mL of dry CH_2Cl_2 were added 0.42 g (1.64 mmol) of *n*-hexadecanoic acid (Aldrich), 5 mg (0.03 mmol) of 4-(dimethylamino)pyridine (Aldrich), and 0.34 g of 1,3-dicyclohexylcarbodiimide (Aldrich). The reaction mixture, protected from moisture ($CaCl_2$), was stirred at room temperature for 3 h. A white precipitate was then filtered off and washed with CH_2Cl_2. The combined organic washings were evaporated under reduced pressure to leave a crude solid that was triturated with ethyl ether and then chromatographed over silica ($CHCl_3$/MeOH 8:2) to afford 0.54 g (75%) of 4-[[2-[[1,2-bis(palmitoyloxy)-3-propyl]dimethylammonio]ethyl]-oxy]-2-[[(tetrahydro-2-pyranyl)oxy]methyl]-6-[(methylthio)methyl]-pyridine bromide, as a white solid: ^1H NMR δ (CD_3OD) 0.90 (br t, 6 H, $(CH_2)_nCH_3$); 1.29 (m, 48 H, $(CH_2)_{12}CH_3$); 1.47–1.97 (m, 10 H, $C(=O)CH_2CH_2(CH_2)_nCH_3$, THP); 2.08 (s, 3 H, SCH_3); 2.40 (m, 4 H, $C(=O)CH_2(CH_2)_nCH_3$); 3.32 (s, 6 H, $N(CH_3)_2$); 3.60 (m, 1 H, THP H_6); 3.79 (s, 2 H, SCH_2Py); 3.85–4.17 (m, 6 H, CH_2NCH_2, THP H_6, H_a $CH_2(O)CH(O)CH_2N$); 4.61–4.92 (m, 6 H, OCH_2Py, NCH_2CH_2O, H_b $CH_2(O)CH(O)CH_2N$, and THP H_2); 5.72 (m, 1 H, $CH_2(O)CH(O)CH_2N$); 7.08 (br s, 2 H, Py, H_3 and H_5).

The protected compound (0.540 g, 0.55 mmol) was dissolved in 50 mL of MeOH and 5 mL of $CHCl_3$. To this solution was added 2 drops of concentrated HCl. After the solution was stirred at room temperature for 20 min, the solvent was evaporated at reduced pressure without heating. The solid thus obtained was dried in vacuo and crystallized from $CHCl_3$/ethyl ether to afford 0.41 (83%) of **2**, as a white solid, mp ≈94 °C (gel), ≈178 °C dec: ^1H NMR δ (1:1 $CDCl_3$:CD_3CN) 0.88 (br t, 6 H, $(CH_2)_nCH_3$); 1.27 (m, 48 H, $C(=O(CH_2CH_2(CH_2)_{12}CH_3)$; 1.59 (m, 4 H, $C(=O)CH_2CH_2(CH_2)_nCH_3$); 2.18 (s, 3 H, SCH_3); 2.32 (m, 4 H, $C(=O)CH_2CH_2(CH_2)_n$); 3.23 (s, 6 H, $N(CH_3)_2$); 3.85–3.93 (m, 4 H, CH_2NCH_2); 4.05 (m, 1 H, H_a $CH_2(O)CH(O)CH_2N$); 4.14 (s, 2 H, SCH_2Py); 4.45 (m, 1 H, H_b $CH_2(O)CH(O)CH_2N$); 4.95 (s, 2 H, OCH_2Py); 5.57 (m, 1 H, $CH_2(O)CH(O)CH_2N$); 7.31 and 7.42 (2 br s, 2 H, Py H_3 and H_5).

Anal. Calcd for $C_{47}H_{87}N_2O_6SBr$: C, 63.56; H, 9.87; N, 3.15. Found: C, 63.16; H, 10.18; N, 3.06.

Vesicle Preparation and Characterization. All vesicle solutions were prepared by dissolving the proper surfactant and, when appropriate, the additive in methylene chloride. The solvent was then evaporated under a gentle nitrogen stream, and 0.05 M MES buffer, pH 6.3 or 5.5, was added. The resulting suspension was sonicated (Artek Sonic Model M150 sonicator, immersion probe, 60% power output) at 50 °C for 20 min. The vesicle solutions were allowed to cool slowly to 25 °C and then filtered through 0.45-μm Millipore filters before use. Gel-to-liquid crystal phase transition temperatures, T_c, were determined from fluorescence polarization[30] studies using covesicallized 1,6-diphenyl-1,3,5-hexatriene (DPH) as a probe under the following conditions: [DPH] = 2.5×10^{-6} M, [surfactant] = 2.5×10^{-4} M.

Ethidium Bromide Trapping. Vesicles suspension made up of surfactant (1.0×10^{-3} M) and ethidium bromide (EB, 5.0×10^{-3} M) were prepared in 0.025 M MES buffer, pH 6.3, and were passed through a Sephadex G-75 column. Sephadex G-75 powder (2.5 g, Pharmacia, Inc.) was allowed to swell overnight in 20 mL of aqueous 0.025 M MES buffer. The resulting slurry was suspended in a 1-cm × 30-cm glass-jacketed chromatography column. The column was then conditioned by passage of 50 mL of buffer. Solutions of EB-loaded vesicles were poured on the column in 5-mL volumes, allowed to absorb, and then eluted with buffer. Fractions of 2.5 mL were collected, and the vesicles were found in fractions 5 to 6, as visualized from light scattering and UV spectroscopy. Free EB was held up by the Sephadex and eluted after fraction 10. The fractions containing vesicles were checked for the presence of entrapped EB using fluorescence spectroscopy (excitation wavelength 480 nm, emission maximum 610 nm). In the case of surfactant **1**, the Sephadex column was performed at 5 °C to prevent leaking of the dye due to a temperature above the phase transition.

(30) Andrich, M. P.; Vanderkooi, J. M. *Biochemistry* **1976**, *14*, 1257.

Kinetic Studies. Solutions were prepared in MES buffer (0.05 M, pH 6.3). No changes in the pH were observed during the kinetic runs. The reactions were followed on a Perkin-Elmer Lambda 5 spectrophotometer equipped, in the case of the fast reactions, with a Hi-Tech stopped-flow accessory. The reaction temperature was maintained at 25 ± 0.1 °C. Kinetics were run under pseudo-first-order conditions ([PNPP] = (1–2) × 10^{-5}), and the release of *p*-nitrophenoxide was followed at 400 nm. The kinetics follow a first-order law even at low ligand concentration. This may be explained with the fact that at this low ligand concentration the amount of ternary complex is no higher than 10–20% of the total amount of PNPP added. Accordingly, a large portion of the substrate is hydrolyzed via the competitive Cu(II)-catalyzed process. The rate constants were obtained by nonlinear regression analysis of the absorbance vs time (using the software package Enzfitter: Leatherbarrow, R. J. *Enzfitter*; Elsevier: Amsterdam, 1987). The fit error of the constants was always less than 1%. The kinetics of PNPP cleavage at different temperatures were followed with an Applied Photophysics SF.17MV stopped-flow spectrometer under the following conditions: [surfactant] = 3.2×10^{-4} M, [Cu^{2+}] = 1.8×10^{-4} M, [PNPP] = 1.0×10^{-5} M, MES 0.05 M, pH 6.3. The kinetics of Cu^{2+} binding were followed with the previous stopped-flow apparatus monitoring the appearance of the surfactant–Cu^{2+} complex absorption band at 320 nm in MES buffer (0.05 M, pH 5.5), the concentrations of surfactant and Cu^{2+} being 5.4×10^{-4} and 3.3×10^{-4} M, respectively. The reaction temperature was maintained at 25 ± 0.1 °C.

Acknowledgment. Support of this research by the "Ministero dell'Universita' e della Ricerca Scientifica e Tecnologica" (MURST) and the National Research Council (CNR)—Progetto Finalizzato "Chimica Fine II"—is gratefully acknowledged. P.S. thanks NATO for financial support (Grant for International Collaboration 0315/87). We are indebted to Professor Robert A. Moss (Rutgers University) for a quite stimulating discussion concerning the results presented in this paper and for disclosing his experiments prior to their publication. Mr. Enzo Castiglione is also thanked for his technical assistance.

Registry No. 1, 141171-42-8; **2**, 141171-43-9; **3**, 122899-69-8; **4**, 141171-44-0; **5**, 70755-47-4; **6**, 141171-45-1; THP, 110-87-2; PPTS, 24057-28-1; DMAP, 1122-58-3; DCC, 538-75-0; CTABr, 57-09-0; Cu, 7440-50-8; $NaSCH_3$, 5188-07-8; n-$C_{16}H_{33}N(CH_3)_2$, 112-69-6; n-$C_{16}H_{33}NH_2$, 143-27-1; CH_3Br, 74-83-9; n-$C_{16}H_{33}NHCH_3$·HCl, 80648-72-2; n-$C_{16}H_{33}NHCH_3$, 13417-08-8; $(i\text{-Pr})_2EtN$, 7087-68-5; n-$C_{16}H_{33}Br$, 112-82-3; n-$C_{15}H_{31}COOH$, 57-10-3; chelidamic acid diethyl ester, 115231-56-6; ethyl 6-(chloromethyl)-4-hydroxy-2-pyridinecarboxylate hydrochloride, 141171-46-2; ethyl 4-hydroxy-6-[(methylthio)methyl]-2-pyridinecarboxylate, 141171-47-3; 2-(hydroxymethyl)-4-hydroxy-6-[(methylthio)methyl]pyridine, 141171-48-4; 18-crown-6, 17455-13-9; benzaldehyde, 100-52-7; *N*-(phenylmethylene)-1-hexadecanamine, 47377-65-1; 4-[[2-(*n*-hexadecylmethylamino)ethyl]oxy]-2-(hydroxymethyl)-6-[(methylthio)methyl]pyridine hydrobromide, 141171-49-5; 3-bromo-1,2-propanediol, 4704-77-2; dimethylamine, 124-40-3; 3-(dimethylamino)-1,2-propanediol hydrobromide, 141171-50-8; 3-(dimethylamino)-1,2-propanediol, 623-57-4; 4-[(2-bromoethyl)oxy]-2-[[(tetrahydro-2-pyranyl)oxy]methyl]-6-[(methylthio)methyl]pyridine, 141171-51-9; 4-[[2-[[1,2-dihydroxy-3-propyl]dimethylammonio]ethyl]-oxy]-2-[[(tetrahydro-2-pyranyl)oxy]methyl]-6-[(methylthio)methyl]-pyridine bromide, 141171-52-0; 4-[[2-[[1,2-bis(palmitoyloxy)-3-propyl]dimethylammonio]ethyl]oxy]-2-[[(tetrahydro-2-pyranyl)oxy]-methyl]-6-[(methylthio)methyl]pyridine bromide, 141171-53-1; *p*-nitrophenyl picolinate, 74104-89-5.

Supplementary Material Available: Figures S1 and S2 (EB trapping experiments), Figures S3 and S4 (fluorescence polarization experiments), Figure S5 (Arrhenius plots), and Figure S6 (rate profiles for the cleavage of PNPP with coaggregates of different additive/ligand ratios) (5 pages). Ordering information is given on any current masthead page.